molbank

MDPI

Short Note

(*E*)-3-[4-(1*H*-Imidazol-1-yl)phenyl]-1-(4-methylphenyl)prop-2-en-1-one

Nicholas Bailey and Bradley O. Ashburn *

Mathematics, Natural, and Health Sciences Division, University of Hawai'i West O'ahu, 91-1001 Farrington Hwy, Kapolei, HI 96707, USA; nmbailey@hawaii.edu
* Correspondence: bashburn@hawaii.edu

Abstract: Imidazole-containing chalcones have been shown to be strongly effective against *Aspergillus fumigatus*, the causative agent for the disease pulmonary aspergillosis. Claisen–Schmidt condensation of 4-(1*H*-imidazol-1-yl)benzaldehyde with 4′-methylacetophenone using aqueous sodium hydroxide in methanol yielded the novel compound (*E*)-3-[4-(1*H*-imidazol-1-yl)phenyl]-1-(4-methylphenyl)prop-2-en-1-one in good yield and purity after recrystallization from hot methanol. With the known antifungal properties of these combined pharmacophores, this novel compound is suitable for anti-aspergillus activity study.

Keywords: chalcone; synthesis; aldol; pulmonary aspergillosis; imidazole

Citation: Bailey, N.; Ashburn, B.O. (*E*)-3-[4-(1*H*-Imidazol-1-yl)phenyl]-1-(4-methylphenyl)prop-2-en-1-one. *Molbank* **2021**, *2021*, M1269. https://doi.org/10.3390/M1269

Academic Editor: Oleg A. Rakitin

Received: 29 April 2021
Accepted: 27 July 2021
Published: 10 August 2021

1. Introduction

Pulmonary aspergillosis (PA) is a spectrum of respiratory diseases that can range from mild to fatal depending on the state of an individual's immune system [1]. Milder manifestations of PA include allergic bronchopulmonary aspergillosis (ABPA), and chronic pulmonary aspergillosis (CPA). These milder forms tend to cause fatigue, difficulty breathing, and hemoptysis [2], while its most lethal diagnosis, invasive aspergillosis (IA), can cause respiratory failure, neurological conditions, and multiorgan failure, depending on where the infection spreads [2]. Named after its infectious agent, the disease stems from the inhalation of conidia of the fungus genus *Aspergillus*.

Aspergillus species are ubiquitous saprophytes and typically inhabit the soil where they recycle essential nutrients from the soil. *Aspergillus'* omnipresence is attributed to its asexual spores called conidia. The conidia are easily propagated, so much so that *Aspergillus* DNA is often found in the lungs of healthy adults [3]. Pulmonary aspergillosis only manifests if the individual who inhales the conidia is immunocompromised [1].

Typically, in the non-immunocompromised host, invasion of *Aspergillus* conidia into the bronchioles and alveoli is eliminated by macrophages and neutrophils [1–4]. Individuals with conditions that compromise these components of the immune system are the most at risk for developing pulmonary aspergillosis. The mortality rate for these individuals ranges from 20% to 90% [1–6], and Bongomin et al. has postulated that there are roughly 3 million cases of CPA worldwide every year. These numbers will only continue to grow if factors such as limited drug therapies, antifungal resistant strains [7,8], and the influx of individuals with compromised immune systems continue. In addition, recent literature illustrates respiratory viruses such as influenza and coronavirus disease 2019 (COVID-19) have led to new classifications of pulmonary aspergillosis, making matters more urgent [9–12].

These classifications are especially disconcerting because they expand the current demographic beyond the immunocompromised. Furthermore, influenza associated aspergillosis (IAA) and COVID-19 associated pulmonary aspergillosis (CAPA) are associated with higher mortality rates and more complications than their counterparts without these

co-infections [9,10]. There seems to be an appreciable prevalence of CAPA (20–30%), especially in mechanically ventilated or severely ill individuals [11]. In particular, one study discovered co-infections of *Aspergillus* in 26% of those with severe ammonia and 40% in those with acute respiratory distress syndrome engendered by COVID-19 [12]. These factors demonstrate that it is imperative to discover new treatments for the evolving disease pulmonary aspergillosis.

Fortunately, pharmacophores like chalcone and imidazoles have shown a wide range of biological activities. These pharmacophores share many pharmacological effects such as anti-inflammatory, antibacterial, anticancer, and antimicrobial activity [13–16]. Recent literature has illustrated that these two pharmacophores in conjunction show potential as an antifungal agent [17,18]. We seek to synthesize similar novel imidazole chalcones as potential treatments for pulmonary aspergillosis.

2. Results

(*E*)-3-[4-(1*H*-Imidazol-1-yl)phenyl]-1-(4-methylphenyl)prop-2-en-1-one **3** was synthesized via a Claisen–Schmidt condensation (Scheme 1). The reaction was performed by adding 4-(1*H*-Imidazol-1-yl)benzaldehyde **1**, 4′-methylacetophenone **2**, and methanol to a round bottom flask at room temperature. Aqueous NaOH was added and allowed to stir for 2 h. The crude product was recrystallized in hot methanol resulting in a yield of 75%.

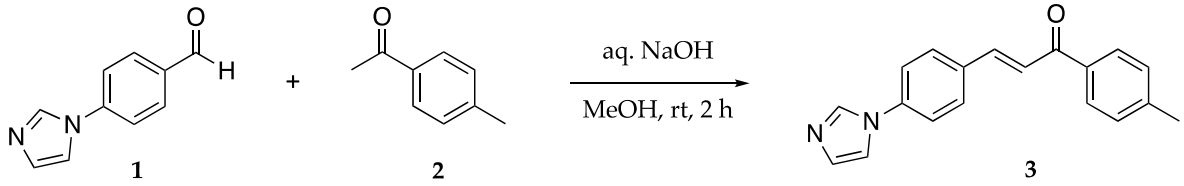

Scheme 1. Claisen-Schmidt condensation to form chalcone **3**.

3. Discussion

The purified compound exhibited spectroscopic signals that confirmed the successful synthesis of chalcone **3**. Using Figure 1 as reference, the ^{1}H-NMR spectrum shows notable confirmatory assignments such as the trans vinylic hydrogens H6 and H7, which were the only two doublets with an integration of one hydrogen. The J value of 15.7 Hz represents the trans alkene geometry. A noteworthy substantiating ^{13}C-NMR signal is the α,β-unsaturated carbonyl peak (C10) at 189.7 ppm being more upfield than a non-conjugated ketone carbonyl. HSQC was then used to assign all carbons bearing protons.

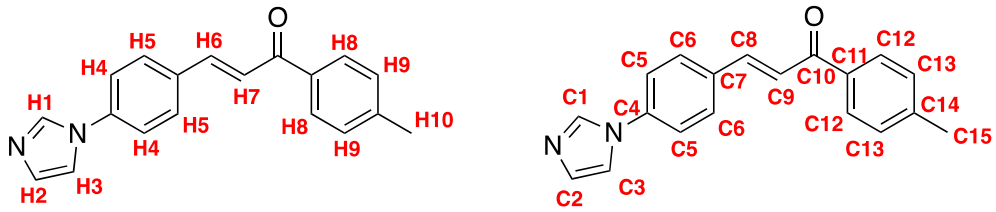

Figure 1. NMR assignment of chalcone **3**.

Assignments from the ^{1}H-NMR and ^{13}C-NMR that were validated by the HSQC were utilized in the HMBC to corroborate other assignments by analyzing the ^{2}J/^{3}J cross peaks. For example, C14 (144.1 ppm) and C13 (129.6 ppm) were verified by their ^{2}J/^{3}J cross peaks with the methyl hydrogens (H10). Additionally, from the carbonyl carbon (C10), cross peaks to H8 (7.98 ppm), H7 (7.54 ppm), and H6 (7.79 ppm) assignments were further established. Chemical shifts of the protons and carbons also were in agreement with predicted anisotropic and resonance effects. The aforementioned signals could then be used to substantiate other signals until all assignments were verified. FT-IR exhibited a sharp carbonyl stretch at 1660 cm^{-1}, which is indicative of an α,β-unsaturated carbonyl.

High resolution mass spectrometry analysis found an M^+ ion at 288.12531 m/z compared to a calculated mass of 288.12626.

4. Materials and Methods

All chemicals, reagents, and solvents used were obtained from commercial sources (Sigma Aldrich, St. Louis, MO, USA and Fisher Scientific, Waltham, MA, USA) and used without further purification. Thin layer chromatography (TLC) was used to monitor reactions and performed using aluminum sheets pre-coated silica gel 60 (HF_{254}, Merck, Waltham, MA, USA), and visualized with UV radiation (Fisher Scientific, Waltham, MA, USA). The product was characterized by ^{1}H-NMR, ^{13}C-NMR, HSQC and HMBC NMR, IR, HRMS, and melting point analysis. Spectra can be found in the supplementary information.

IR spectra were recorded on a ThermoFisher iS5 FT-IR. Melting point was determined in open capillaries using a Stuart SMP3 melting point apparatus. ^{1}H and ^{13}C-NMR spectra were collected using a 500 MHz Bruker AV-500 NMR spectrometer. HSQC and HMBC were collected using a 600 MHz Agilent DD2 600 MHz NMR spectrometer. Spectra were referenced to residual $CHCl_3$. Chemical shifts were quoted in ppm and coupling constants (J) were recorded in hertz (Hz). High resolution mass spectrum was acquired using an Agilent Technologies Series 6200 TOF spectrometer.

A solution of aqueous NaOH (0.25 mL, 3.75 mmol, 15 M) was added to a round bottom flask containing 4-(1*H*-imidazol-1-yl)benzaldehyde **1** (0.430 g, 2.50 mmol), 4′-methylacetophenone **2** (0.335 g, 2.50 mmol), and methanol (7.5 mL). The mixture was stirred at room temperature for 2 h (monitored by TLC in 5% dichloromethane/hexanes and visualized with UV radiation) during which a yellow-white precipitate formed. The mixture was diluted with water (10 mL) then cooled to 0 °C, and collected *in vacuo*, washed twice with an ice-cold solution of 10% methanol/H_2O (5 mL portions). The crude product was purified by recrystallization from hot methanol to yield pure chalcone **3** as light yellow crystals (0.543 g, 1.88 mmol, 75%).

(*E*)-3-[4-(1*H*-Imidazol-1-yl)phenyl]-1-(4-methylphenyl)prop-2-en-1-one (**3**): mp 171–172 °C; ^{1}H-NMR ($CDCl_3$, 500 MHz): 7.93 ppm (2H, d, J = 8.2 Hz, H8), 7.90 ppm (1H, s, H1), 7.79 ppm (1H, d, J = 15.7 Hz, H6), 7.73 ppm (2H, d, J = 8.5 Hz, H5), 7.54 ppm (1H, d, J = 15.7 Hz, H7), 7.43 ppm (2H, d, J = 8.6 Hz, H4), 7.30 ppm (2H, d, J = 8.4 Hz, H9), 7.30 ppm (1H, s, H2), 7.22 ppm (1H, s, H3), 2.42 ppm (3H, s, H10); ^{13}C-NMR ($CDCl_3$, 125 MHz): 186.7 ppm (C10), 144.1 ppm (C14), 142.7 ppm (C8), 138.7 ppm (C4), 135.6 ppm (C11), 135.5 ppm (C1), 134.4 ppm (C7), 131.0 ppm (C3), 130.1 ppm (C6), 129.6 ppm (C13), 128.8 ppm (C12), 122.9 ppm (C9), 121.6 ppm (C5), 118.0 ppm (C2), 21.8 ppm (C15); FT-IR (KBr) 3167 cm^{-1} (C-H_{Ar}), 3117 cm^{-1} (C-H_{Ar}), 3041 cm^{-1} (C-H_{Ar}), 1660 cm^{-1} (C=O), 1597 cm^{-1} (C=C), 1518 cm^{-1} (C=C); HRMS m/z calc for $C_{19}H_{16}N_2O$ is 288.12626; found 288.12531.

Supplementary Materials: The following are available online: Copies of the ^{1}H, ^{13}C-NMR, HSQC, HMBC, IR, and HRMS spectra.

Author Contributions: Conceptualization, B.O.A.; methodology, B.O.A.; investigation, B.O.A. and N.B.; writing—original draft preparation, B.O.A. and N.B.; writing—review and editing, B.O.A. and N.B.; All authors have read and agreed to the published version of the manuscript.

Funding: This project was supported by grants from the National Institutes of Health (NIH), National Institute of General Medical Sciences (NIGMS), IDeA Networks of Biomedical Research Excellence (INBRE), Award number: P20GM103466. The content is solely the responsibility of the authors and does not necessarily represent the official views of the National Institutes of Health.

Institutional Review Board Statement: Not applicable.

Informed Consent Statement: Not applicable.

Data Availability Statement: The data presented in this study are available in the Supplemental Materials.

Conflicts of Interest: The authors declare no conflict of interest.

References

1. Dagenais, T.R.T.; Keller, N.P. Pathogenesis of *Aspergillus fumigatus* in Invasive Aspergillosis. *Clin. Microbiol. Rev.* **2009**, *22*, 447–465. [CrossRef] [PubMed]
2. Bazaz, R.; Dening, D.W. Aspergillosis: Cause, types and treatment. *Pharm. J.* **2019**, *303*, 7927.
3. Latgé, J.P.; Chamilos, G. *Aspergillus fumigatus* and Aspergillosis in 2019. *Clin. Microbiol. Rev.* **2019**, *33*, e00140-18. [CrossRef] [PubMed]
4. Tischler, B.Y.; Hohl, T.M. Menacing Mold: Recent Advances in Aspergillus Pathogenesis and Host Defense. *J. Mol. Biol.* **2019**, *431*, 4229–4246. [CrossRef] [PubMed]
5. Bongomin, F.; Gago, S.; Oladele, R.O.; Denning, D.W. Global and Multi-National Prevalence of Fungal Diseases—Estimate Precision. *J. Fungi* **2017**, *3*, 57. [CrossRef] [PubMed]
6. Vuong, M.F.; Waymack, J.R. Aspergillosis. In *StatPearls*; StatPearls Publishing: Treasure Island, FL, USA, 2020.
7. Rudramurthy, S.M.; Paul, R.A.; Chakrabarti, A.; Mouton, J.W.; Meis, J.F. Invasive Aspergillosis by *Aspergillus flavus*: Epidemiology, Diagnosis, Antifungal Resistance, and Management. *J. Fungi* **2019**, *5*, 55. [CrossRef] [PubMed]
8. Romero, M.; Messina, F.; Marin, E.; Arechavala, A.; Depardo, R.; Walker, L.; Negroni, R.; Santiso, G. Antifungal Resistance in Clinical Isolates of *Aspergillus spp*.: When Local Epidemiology Breaks the Norm. *J. Fungi* **2019**, *5*, 44. [CrossRef] [PubMed]
9. Waldeck, F.; Boroli, F.; Suh, N.; Garcia, P.D.W.; Flury, D.; Notter, J.; Iten, A.; Kaiser, L.; Schrenzel, J.; Boggian, K.; et al. Influenza-Associated Aspergillosis in Critically-Ill Patients a Retrospective Bicentric Cohort Study. *Eur. J. Clin. Microbiol. Infect. Dis.* **2020**, *39*, 1915–1923. [CrossRef] [PubMed]
10. Marr, K.A.; Platt, A.; Tornheim, J.A.; Zhang, S.X.; Datta, K.; Cardozo, C.; Garcia-Vidal, C. Aspergillosis Complicating Sever Coronavirus Disease. *Emerg. Infect. Dis.* **2021**, *27*, 18–25. [CrossRef] [PubMed]
11. Kuehn, B.M. Pulmonary Fungal Infections Affect Patients With COVID-19. *JAMA* **2020**, *324*, 2248. [PubMed]
12. Steenwyk, J.L.; Mead, M.E.; Castro, P.A.; Valero, C.; Damasio, A.; Santos, R.A.C.; Labella, A.L.; Li, Y.; Knowles, S.L.; Raja, H.A.; et al. Genomic and Phenotypic Analysis of COVID-19-Associated Pulmonary Aspergillosis isolates of *Aspergillus fumigatus*. *bioRxiv* **2020**. [CrossRef]
13. Zhuang, C.; Zhang, W.; Sheng, C.; Zhang, W.; Xing, C.; Miao, Z. Chalcone: A Privileged Structure in Medicinal Chemistry. *Chem. Rev.* **2017**, *117*, 7762–7810. [CrossRef]
14. Zheng, X.; Ma, Z.; Zhang, D. Synthesis of Imidazole-Based Medicinal Molecules Utilizing the van Leusen Imidazole Synthesis. *Pharmaceuticals* **2020**, *13*, 37. [CrossRef] [PubMed]
15. Bailey, N.; Atanes, A.; Ashburn, B.O. (E)-3-(4-chlorophenyl)-1-(2-fluoro-4-methoxyphenyl)-2-propen-1-one. *Molbank* **2021**, *2021*, M1184. [CrossRef]
16. Amato-Ocampo, J.; Carrillo, R.; Kae, H.; Ashburn, B.O. Synthesis and Antimicrobial Evaluation of a Series of Chlorinated Chalcone Derivatives. *IJPPR Human* **2018**, *13*, 112–119.
17. Hussain, T.; Zia-ur-Rehman, M.; Zaheer, M.; Ashraf, M.; Bolte, M. 1-[4-(1H-Imidazol-1-yl)phenyl]-3-phenylprop-2-en-1-ones—A potential pharmacophore bearing anti-leishmanial activity. *J. Chem. Res.* **2016**, *40*, 199–204. [CrossRef]
18. Hussain, T.; Siddiqui, H.L.; Zia-ur-Rehman, M.; Yasinzai, M.M.; Parvez, M. Anti-oxidant, anti-fungal and nti-leishmanial activities of novel 3-[4-(1H-imidazol-1-yl) phenyl]prop-2-en-1-ones. *Eur. J. Med. Chem.* **2009**, *40*, 4654–4660. [CrossRef] [PubMed]